



Cite this: *New J. Chem.*, 2020, **44**, 14306

Synthesis, structural and toxicological investigations of quarternary phosphonium salts containing the P-bonded bioisosteric CH₂F moiety†

Marco Reichel,  Cornelia Unger,  Sviatlana Dubovnik, Andreas Roidl, Andreas Kornath  and Konstantin Karaghiosoff *

Tertiary alkyl, aryl or amino phosphines PR₃ (R = Me, *n*Bu, C₂H₄CN, NEt₂) and the bis[(2-diphenylphosphino)phenyl]ether (POP) were allowed to react with fluoroiodomethane to produce fluoromethyl phosphonium salts in yields between 60–99%. The compounds were characterized by vibrational and NMR spectroscopy and in most cases also by single crystal X-ray diffraction. Diphenyl(fluoromethyl) phosphine was synthesized as a mixed aryl–alkyl-phosphine and the TEP value (Tolman electronic parameter) was determined in order to explain its low reactivity. The molecular and crystal structures of the new fluoromethyl phosphonium salts [R₃PCH₂F]I with R = Me, C₂H₂CN and NEt₂ as well as of the salt resulting from the fluoromethylation of POP provided additional information on the structural behavior of the bioisoster CH₂F group bonded to phosphorus. Hydrogen bonding in the crystal is compared with that observed in the crystal structure of PPh₃CH₂FI. The toxicity of the sufficiently water soluble salt [Me₃PCH₂F]I was investigated and the toxicological effect of the CH₂F group was compared to that of the bioisoster CH₂OH group in THPS.

Received 7th May 2020,
Accepted 2nd August 2020

DOI: 10.1039/d0nj02310h

rsc.li/njc

Introduction

Phosphonium salts are a long known class of compounds and widely used by chemists, *e.g.* as starting materials for Wittig reactions.¹ Fluoromethyl phosphonium salts have been described to serve as precursors for the synthesis of fluoroolefines,² and have also been employed to simple transfer the fluoromethyl group to other substrates.³ This property of fluoromethyl phosphonium salts is particularly interesting for the preparation of biological active compounds, due to the bioisosteric properties of the CH₂F group.^{3b,4} In the course of our recent systematic investigations on fluoromethylating agents we experienced that very little is known on the structural properties of CH₂F bonded to phosphorus.^{3a} This prompted us to investigate some more phosphonium salts, containing the PCH₂F structural motif. In addition to the fluoromethylating ability and the use for the synthesis of fluoroolefines the biological activity and in particular the toxicity of fluoromethyl phosphonium salts is of interest.⁵ It is known that phosphonium salts containing the bioisosteric CH₂OH group can have a biocidal effect on biofilms and in particular

tetrakis(hydroxymethyl)phosphonium sulfate (THPS) is widely used as biocide in oil pipelines and/or oil fields as well as in the paper producing industry against Gram negative bacteria.⁶ Considering the opposite charges of phosphonium cations and Gram negative bacteria, it is not surprising that the mechanism of interaction is based on a strong electrostatic interaction. The mode of action can be described in such a way, that the proteins of the membrane wall of the bacteria will react with the CH₂OH groups of THPS to form CH₂NR₂ with cleavage of water. This event damages the structure of the bacteria and as consequence nonspecific increase of cell permeability or abnormal morphology cause lysis (Fig. 1).⁷

It is already known from warfare agents of the G series (sarin, cyclosarin, soman) that also strong element fluorine bonds can be cleaved by organisms under formation of HF.⁸ This prompted us to investigate, the toxicity of the most water soluble phosphonium salt, [Me₃PCH₂F]I, in particular regarding a possible cleavage of the C–F bond on hydrolysis under biological conditions with formation of toxic HF.

Results and discussion

The new trifluoromethyl phosphonium salts 1–5 were prepared by reaction of the respective phosphines with CH₂FI (Scheme 1).

Department Chemie, Ludwig-Maximilian-Universität, Butenandstr. 5-13 (D), 81377 München, Germany. E-mail: Konstantin.Karaghiosoff@cup.uni-muenchen.de

† Electronic supplementary information (ESI) available: Copies of NMR spectra and X-ray details. CCDC 1967513–1967517. For ESI and crystallographic data in CIF or other electronic format see DOI: 10.1039/d0nj02310h

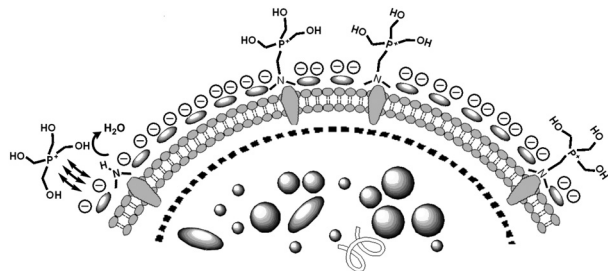


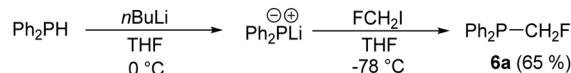
Fig. 1 Mechanism of interaction and mode of action of THPS with the cell wall of Gram negative bacteria.

The phosphonium salts 1–5 are isolated as colorless crystalline air stable solids. Except for 1 they are quite poorly soluble in water and readily soluble in polar aprotic solvents like MeCN, DCM or THF.

The challenge of phosphine fluoromethylation with CH_2FI is represented by the reaction rate, which is in part quite slow, and by the choice of proper reaction conditions. In fact, already small deviation from the selected reaction conditions lead to the formation of byproducts, which are difficult to separate. In general fluoromethylation with CH_2FI is more difficult than methylation with CH_3I .⁹ Reaction time, necessary for complete reaction, strongly depends on the substituents at phosphorus. Fluoromethylation is fast (0.5 h/−78 °C) in the case of Me_3P and much slower in the case of $n\text{Bu}_3\text{P}$ (32 h/35 °C) or bis(phosphine) POP (24 h/110 °C). Thus the electron donor ability of the phosphine seems to play an important role. Considering the long reaction time needed for the fluoromethylation of triphenyl phosphine the reaction of the new alkyl/aryl substituted fluoromethyl diphenylphosphine 6 with CH_2FI was investigated. Phosphine 6 is readily prepared starting from diphenylphosphine by lithiation and subsequent fluoromethylation with CH_2FI (Scheme 2). Unfortunately, further reaction of 6 with CH_2FI under different conditions did not yield the corresponding bis(fluoromethyl) phosphonium salt. Either no reaction or the formation of several unidentified phosphorus containing products at elevated temperatures was observed.

In order to characterize the phosphine 6 with respect to its donor ability its Tolman electronic parameter (TEP) was determined (Fig. 2).¹⁰ In the series of phosphines the donor properties for 6 are similar to those for Ph_2PMe and Ph_3P , which explains its low tendency to form the phosphonium salt.

The fluoromethyl phosphonium salts 1–5 have lower melting points and lower decomposition temperatures as compared to the



Scheme 2 Synthesis of fluoromethyl diphenylphosphine 6a.

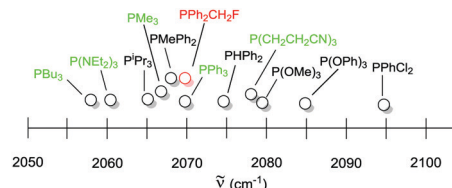


Fig. 2 TEP value of $\text{PPh}_2\text{CH}_2\text{F}$ compared to the used and common phosphines.

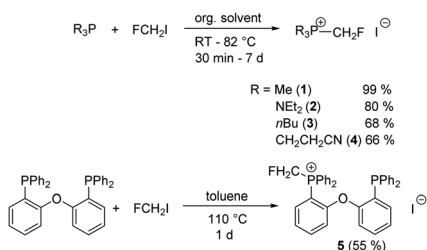
corresponding methyl derivatives.¹¹ The same trend has been reported for $[\text{Ph}_3\text{PCH}_2\text{F}]\text{BF}_4$ as compared to $[\text{Ph}_3\text{PCH}_3]\text{BF}_4$.¹²

While the ^{31}P chemical shifts of the phosphonium salts 1–5 reflect also the influence of the other three substituents at phosphorus the P-bonded CH_2F group displays characteristic ^1H , ^{13}C and ^{19}F chemical shifts and coupling constants (Table 1).

The ^1H , ^{13}C and ^{19}F NMR signals of P- CH_2F in 1–5 are typically found in the quite narrow ranges of 5–6 ppm, 76–78 ppm and −240 to −250 ppm, respectively. Also for the coupling constants $^1J_{\text{CF}}$ (180–190 Hz), $^2J_{\text{PF}}$ (50–60 Hz) and $^2J_{\text{FH}}$ (44–46 Hz) characteristic ranges are observed. The coupling of phosphorus to the proton of CH_2F is very small (<1 Hz), in contrast to $^2J_{\text{PH}}$ to the protons of the other alkyl substituents at phosphorus in 3 and 4.

Only in the case of 1 a $^2J_{\text{PH}}$ coupling of 1.6 Hz to the CH_2 protons of CH_2F was clearly observed. This effect is obviously due to the fluorine atom, as impressively shown by the ^{31}P NMR spectrum of 1 (Fig. 3, top). Coupling of phosphorus to the methyl protons (15.0 Hz) is much larger than $^2J_{\text{PH}}$ to the methylene protons (1.6 Hz); both are smaller than $^2J_{\text{PF}}$ of 45.3 Hz. These couplings cause splitting of the ^{31}P NMR signal of 1 to the well resolved multiplet shown in Fig. 3 (top). In the ^{19}F NMR spectrum of 1 a doublet of triplets due to coupling of ^{19}F with ^{31}P and with ^1H of the CH_2F group is observed. Each of the resulting six lines is further splitted by long range coupling of ^{19}F to ^1H of the methyl groups over four bonds (Fig. 3 bottom). The NMR data of the CH_2F group fit well to those reported for $[\text{Ph}_3\text{PCH}_2\text{F}]\text{BF}_4$.¹³

Single crystals, suitable for X-ray diffraction studies were obtained for compounds 1, 2, 4 and 5. Compound 1 crystallizes



Scheme 1 Synthesis of fluoromethylphosphonium iodides 1–5.

Table 1 Chemical shifts and coupling constants for the CH_2F group in the fluoromethyl phosphonium salts 1–5

	Chemical shift			Coupling constant		
	^1H	^{13}C	^{19}F	$^1J_{\text{C,F}}$	$^2J_{\text{P,F}}$	$^2J_{\text{F,H}}$
1	5.44	77.1	−242	183.8	60.3	45.3
2	5.77	78.2	−241	182.6	59.9	45.9
3	5.92	76.1	−247	190.4	51.6	45.9
4	5.85	76.8	−249	188.3	56.8	44.8
5	6.28	—	−240	—	62.2	46.0
6	5.28	84.6	−230	199.9	114.0	49.0

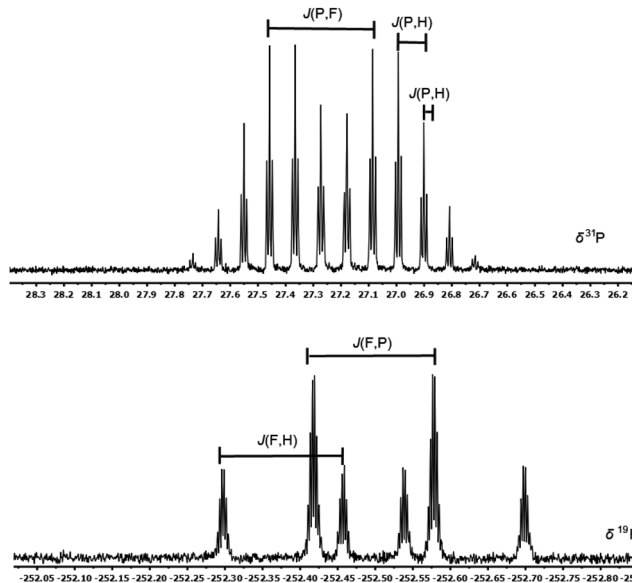


Fig. 3 ^{31}P NMR spectrum (top) and ^{19}F NMR spectrum (bottom) of **1** in CDCl_3 .

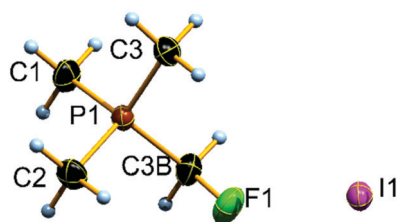


Fig. 4 Molecular structure of compound **1** in the crystal; DIAMOND representation,²⁸ thermal ellipsoids are shown at 50% probability level. The CH_2F group is disordered over two positions; only one of the positions is shown.

in the orthorhombic space group $Pnma$ with one formula unit in the unit cell. The asymmetric unit is shown in Fig. 4. The fluoromethyl group is disordered almost equally over two positions. The phosphorus displays a tetrahedral surrounding. The P,C distance to the CH_2F group (1.792(2) Å) compares well to that in the tetramethyl phosphonium cation (1.783(2) Å).¹⁴ and seems to be somewhat shorter as compared to the corresponding distance in $[\text{Ph}_3\text{PCH}_2\text{F}]\text{I}$ (1.810(4) Å)^{3a} and to the P,C distance in $\text{P}(\text{CH}_2\text{OH})_4^+$ (1.809(6) Å).¹⁵

The C,F bond length (1.369(5) Å) is in the expected range.^{3a,14a} In the crystal weak interactions involving the iodide anion and the fluorine atom are observed (Fig. 5).

A weak hydrogen bond $\text{F}\cdots\text{H}$ (2.489(4) Å)¹⁶ between the fluorine atom and one of the methyl hydrogen atoms of a second phosphonium cation leads to the formation of chains. Similar interactions have been reported also for the crystal structure of $\text{Ph}_3\text{PCH}_2\text{FI}$.^{3a} The iodide anions are located between the chains and display weak $\text{I}\cdots\text{H}$ interactions (3.14(2) Å)¹⁷ to hydrogen atoms of the CH_2F group (Fig. 5).

Compound **2** crystallizes in the triclinic space group $P\bar{1}$ with two formula units in the asymmetric unit (Fig. 6).

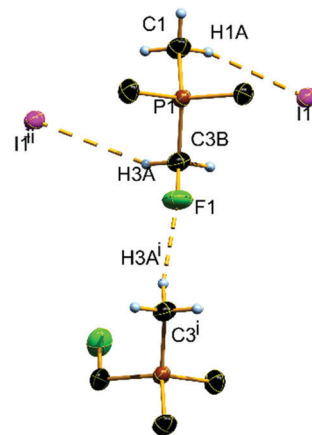


Fig. 5 Hydrogen bonding in the crystal structure of compound **1**. Only one of the two positions of the CH_2F group and only the relevant hydrogen atoms are shown. DIAMOND representation,²⁸ thermal ellipsoids are shown at 50% probability level. Symmetry code: i: $1 - x, 1 - y, 1 - z$; ii: $-0.5 + x, 0.5 - y, 0.5 - z$.

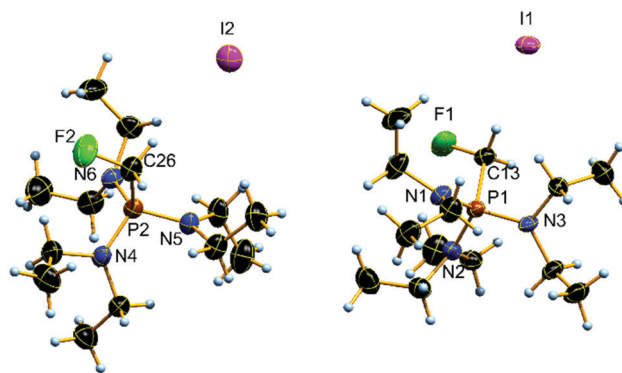


Fig. 6 Molecular structure of compound **2** in the crystal, DIAMOND representation,²⁸ thermal ellipsoids shown at 50% probability level.

The phosphorus atom shows a distorted tetrahedral surrounding, similar to that observed in the $\text{P}(\text{NEt}_2)_3\text{CH}_3^+$ cation.¹⁸ The ethyl units are twisted with respect to each other. While the C13–F1 (1.378(4) Å) and C26–F2 (1.393(4) Å) distances are in the expected range, the P1–C13 (1.824(3) Å) and P2–C26 (1.813(4) Å) distances are elongated as compared to those in the $\text{P}(\text{NEt}_2)_3\text{CH}_3^+$ cation (1.783(3) Å)¹⁸ and in **1**.

Similar to **1**, compound **2** also shows weak intermolecular $\text{CH}\cdots\text{F}$ and $\text{CH}\cdots\text{I}$ interactions (Table 2), as already reported for $[\text{PPh}_3\text{CH}_2\text{F}]\text{I}$.^{3a,16} The $\text{CH}\cdots\text{F}$ interactions (Fig. 7) favour an arrangement of the cations in the crystal to form chains, which are interconnected by the iodide anions through $\text{CH}\cdots\text{I}$ hydrogen bonds.

Compound **4** crystallizes in the monoclinic space group $P21/c$. The asymmetric unit is shown in Fig. 8.

Atom distances and bond angles of phosphonium salt **4** are as expected. The C1–F1 distance (1.384(2) Å) compares well to those found for the fluoromethyl phosphonium salts **1** and **2** and seems to stay unaffected by the other substituents at phosphorus.

Table 2 Structural parameters of the hydrogen bonds in the crystals of compounds **1**, **2**, **4** and **5**; bond lengths in Å, bond angles in °

Compound	Bond	$d(\text{D-H})$	$d(\text{H}\cdots\text{A})$	$d(\text{D}\cdots\text{A})$	$\angle(\text{D-H}\cdots\text{A})$
1	C3B-H3A \cdots I1 ⁱⁱ	0.99(2)	3.14(2)	4.026(3)	149.7(2)
	C1-H1A \cdots I1	0.98(2)	3.02(2)	3.951(4)	159.7(3)
2	C3 ⁱ -H3A ⁱ \cdots F1	0.98(3)	2.48(4)	3.436(4)	162.6(2)
	C13-H13A \cdots I1	0.99(2)	2.92(2)	3.901(4)	178(2)
	C13-H13B \cdots I1 ⁱ	0.99(2)	3.13(2)	4.084(4)	164(1)
4	C25 ⁱⁱ -H25 ⁱⁱ \cdots F1	0.98(2)	2.47(3)	3.324(6)	144.4(4)
	C1-H1A \cdots I1 ⁱⁱ	0.92(2)	3.13(9)	3.841(2)	91.6(7)
5	C9 ⁱ -H9A ⁱ \cdots F1	0.96(2)	2.46(1)	3.348(3)	153.4(8)
	C1-H1B \cdots F1 ⁱ	0.94(2)	2.68(2)	3.482(2)	143(1)
6b	C1-H1A \cdots I1	0.94(2)	2.95(2)	3.863(3)	165(1)
	O2-H211 \cdots I1	0.88(2)	2.7(2)	3.45(2)	146(2)
	C32 ⁱ -H32 ⁱ \cdots F1	0.95(2)	2.60(2)	3.465(4)	152(2)
	C44 ⁱ -H44 ⁱ \cdots F1	0.96(3)	2.42(2)	3.181(3)	137(2)
	C6-H6 \cdots F1	0.97(3)	2.75(3)	3.250(3)	113(2)

Symmetry code: (**1**) i: $1-x, 1-y, 1-z$; ii: $-0.5+x, 0.5-y, 0.5-z$; (**2**) i: $1-x, 1-y, -z$; ii: $1-x, 1-y, 1-z$; (**4**) i: $1-x, -0.5+y, 1.5-z$; ii: $1-x, 1-y, 1-z$; (**5**) i: $-x, 1-y, 1-z$; (**6b**) i: $-x, 1-y, 1-z$.

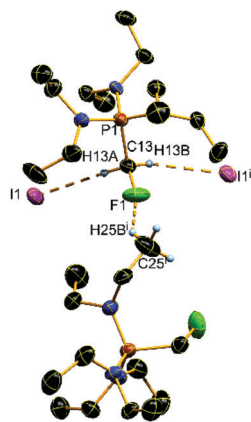


Fig. 7 Hydrogen bonding in the crystal structure of compound **2**. Only the relevant hydrogen atoms are shown. DIAMOND representation,²⁸ thermal ellipsoids shown at 50% probability level. Symmetry code: i: $1-x, 1-y, -z$; ii: $1-x, 1-y, 1-z$.

In the crystal weak intermolecular CH \cdots F interactions between the CH₂CN hydrogen atoms and fluorine as well as CH \cdots I interactions between the CH₂F hydrogen atoms and the iodide anions are observed (Fig. 9). They result in a similar arrangement of cations and anions as found for phosphonium salts **1** and **2**.

Phosphonium salt **5** crystallizes in the triclinic space group $P\bar{1}$. The asymmetric unit, shown in Fig. 10 contains one molecule of water which position is occupied by a third.

The phosphorus atom P1 in the cation of **5** carrying the CH₂F group displays a distorted tetrahedral environment, while the arrangement around P2 is pyramidal (sum of CPC angles 304.3°). As expected, CPC angles at P2 (100.6(2)–102.3(2)°) are smaller as compared to CPC angles at P1 (108.6(2)–111.4(2)°). The aryl substituents at both phosphorus atoms are rotated around the PC-axis to adopt a propeller-like arrangement. Atom distances and bond angles of the P-CH₂F unit fit well to those found for the fluoromethyl phosphonium salts **1**, **2** and **4**.

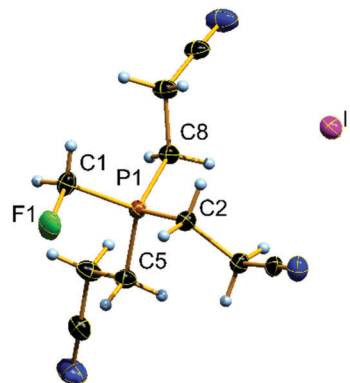


Fig. 8 Molecular structure of compound **4** in the crystal; DIAMOND representation,²⁸ thermal ellipsoids drawn at 50% probability level.

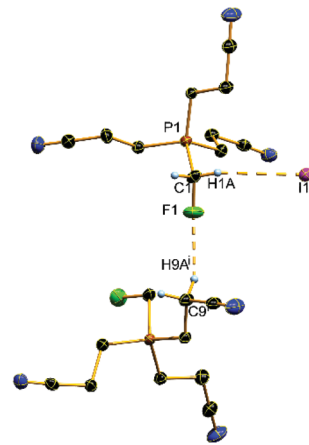


Fig. 9 Hydrogen bonding in the crystal structure of compound **4**. Only the relevant hydrogen atoms are shown. DIAMOND representation,²⁸ thermal ellipsoids shown at 50% probability level. Symmetry code: i: $1-x, -0.5+y, 1.5-z$; ii: $1-x, 1-y, 1-z$.

In the crystal the arrangement of cations and anions is governed by weak OH \cdots I, CH \cdots I and CH \cdots F hydrogen bonds (Fig. 11 and Table 2). Weak CH \cdots F interactions favor the formation of dimers and involve one hydrogen atom of each CH₂F group. The second hydrogen atom undergoes CH \cdots I hydrogen bonding to one iodide anion. The resulting aggregates are partially interconnected by OH \cdots I hydrogen bonds. In order to obtain a more precise analysis of the intermolecular interactions in the crystal of the fluoromethyl phosphonium salts, fingerprint plots and Hirshfeld surfaces were created for compounds **2**, **4** and **5**. Phosphonium salt **1** has been omitted due to the disorder in the crystal. The red dots on the Hirshfeld surfaces indicate contacts between layers (Fig. 12).

The sum $d_i + d_e$ (d_i : distance from the Hirshfeld surface to the nearest atom interior; d_e : distance from the Hirshfeld surface to the nearest atom exterior) indicates that all H \cdots I interactions in the structures of **2**, **4** and **5** are weak. As can be seen from the width of the flanks in plots (a)–(c) (Fig. 12) the number of hydrogen bonds to I Γ decrease in the order $4 > 2 > 5$. The more pronounced spikes for H \cdots F contacts in the case of **4**

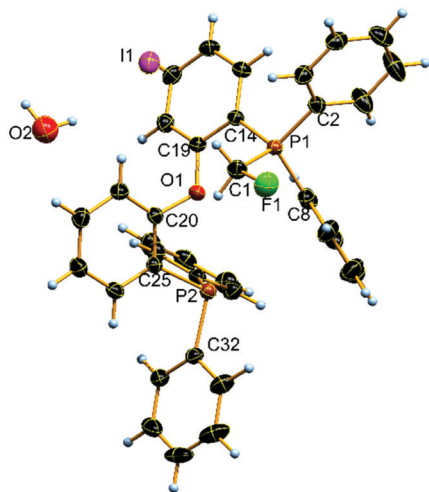


Fig. 10 Molecular structure of compound **5** in the solid state DIAMOND representation,²⁸ thermal ellipsoids shown at 50% probability level. Water position is only occupied by a third.

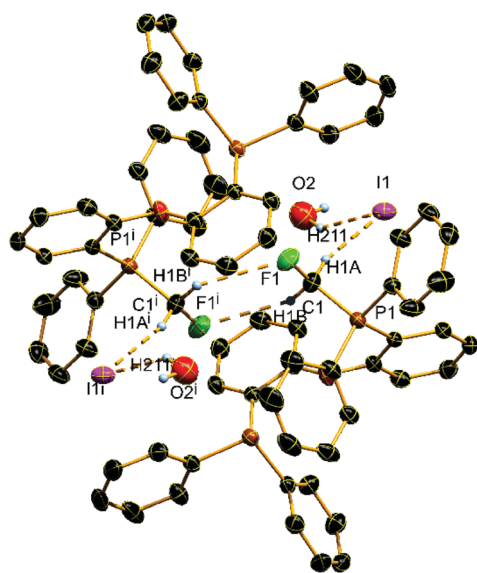


Fig. 11 Hydrogen bonding in the crystal structure of compound **5**. Only the relevant hydrogen atoms are shown. DIAMOND representation,²⁸ thermal ellipsoids shown at 50% probability level. Symmetry code: $i: -x, 1 - y, 1 - z$. The position of the water molecule displays a 30% occupancy.

(plot b), Fig. 12) indicate for this compound the greatest number of hydrogen bonds involving fluorine. The absence of such spikes in the case of **5** (plot c), Fig. 12) is representative for less H...F interactions in the crystal, which is in accord with the formation of dimers. The sum of $d_i + d_e$ also shows, that the H...F interactions are weak.

A single crystal of (fluoromethyl)diphenyl phosphine oxide (**6b**),^{19a} suitable for X-ray diffraction, was collected from an NMR tube originally containing the phosphine dissolved in CDCl₃. The compound crystallizes in the space group $P\bar{1}$ with four crystallographically independent molecules in the asymmetric unit (Fig. 13).

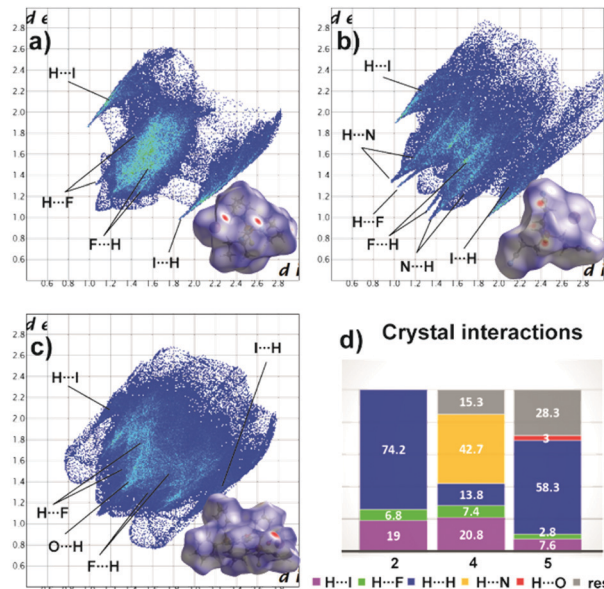


Fig. 12 Two dimensional fingerprint plot and the corresponding Hirshfeld surface (bottom right in 2D plot) for **2** (a), **4** (b) and **5** (c). Color coding: white, distance d equals vdW distance; blue, d exceeds VdW distance, red, d , smaller than VdW distance). Population of close contacts of **2**, **4** and **5** in crystal is shown in plot d).

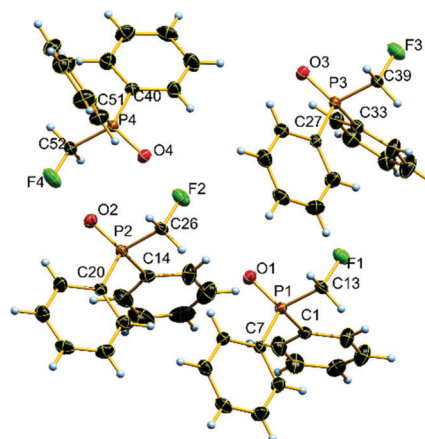


Fig. 13 Molecular structure of (fluoromethyl)diphenyl phosphine oxide in the crystal. DIAMOND representation,²⁸ thermal ellipsoids shown at 50% probability level.

The phosphorus atom shows in all four molecules a distorted tetrahedral arrangement of the substituents. The phenyl groups are slightly twisted against each other. The P-CH₂F distances (P1-C13: 1.815(2) Å; P2-C26: 1.817(2) Å; P3-C39: 1.813(2) Å; P4-C52 (1.817(2) Å) are slightly elongated as compared to that in diphenylmethyl phosphine oxide (1.790(3) Å)^{19b} and similar to that reported for diphenyl hydroxymethyl phosphine oxide (1.816(2) Å).²⁰ The C-F bonds (C13-F1: 1.398(2) Å; C26-F2: 1.393(2) Å; C39-F3: 1.390(2) Å; C52-F4: 1.383(3) Å) fit well to those observed for the phosphonium salts **1**, **2** and **4** and are obviously not influenced by phosphorus coordination. In the crystal one intramolecular and two weak intermolecular

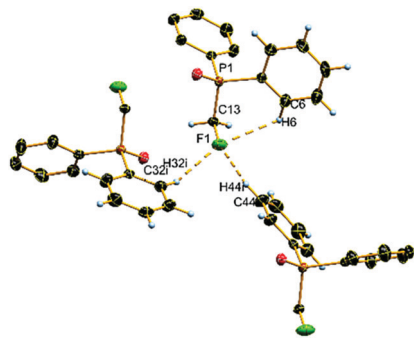


Fig. 14 Hydrogen bonding in the crystal structure of fluoromethyl diphenyl phosphine oxide. For a better overview, H atoms were partially omitted. DIAMOND representation,²⁸ thermal ellipsoids shown at 50% probability level. Symmetry code: $i: -x, 1 - y, 1 - z$.

H \cdots F contacts to aromatic CH hydrogen atoms are observed (Fig. 14 and Table 2).

However, the intermolecular F \cdots H interactions, which according to a Hirshfeld analysis represent 12.4% of all intermolecular interactions in the crystal of **6b**, are more numerous than observed for **2**, **4** or **5** (Fig. 12d).

In order to find out whether the phosphorus bonded CH₂F unit can react with the membrane proteins in analogy to the bioisosteric P-CH₂OH group (Fig. 1), it was first necessary to choose a suitable phosphonium salt. Solubility tests showed that only compound **1** is sufficiently soluble in water to perform such tests. Sodium iodide (EC₅₀: 289.61) was measured to rule out that a possible inhibition was caused by the iodide anion. Tetramethyl phosphonium iodide was also included in the investigations to determine whether the phosphonium cation itself already has an inhibition effect on bacteria. The inhibitory effect of water samples on the light emission of Gram negative *Vibrio fischeri* bacteria,²¹ shows clear differences for compound **1**, [PMe₄]I and THPS ([P(CH₂OH)₄]SO₄) (Fig. 15). For classification of the toxicity the compounds with EC₅₀ values lower than 0.10 g L⁻¹ are categorized as very toxic while compounds with EC₅₀ values between 0.10 g L⁻¹ and 1.00 g L⁻¹ are rated as toxic and above 1.00 g L⁻¹ as less

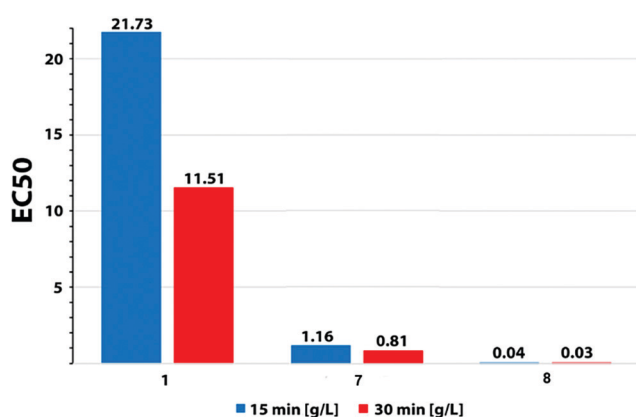


Fig. 15 EC₅₀ values for [PMe₃CH₂F]I (**1**), [PMe₄]I (**7**), and [P(CH₂OH)₄]SO₄ (**8**) measured after 15 min (blue) and after 30 min (red).

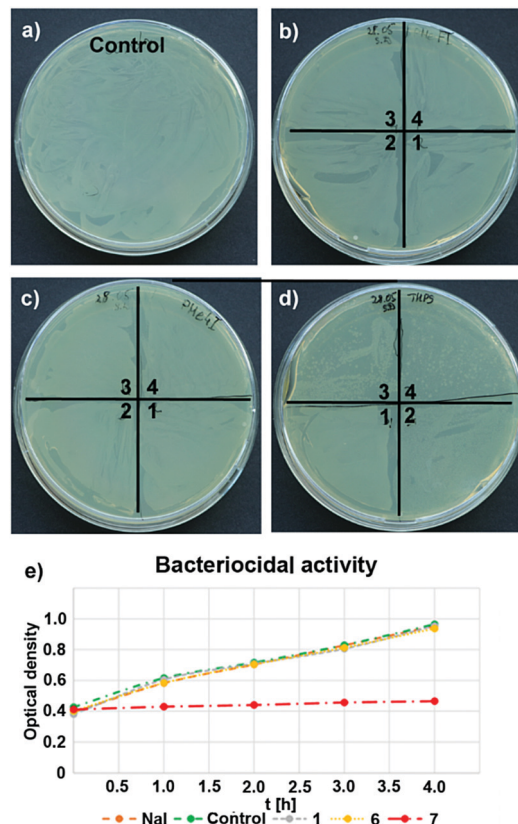


Fig. 16 *E. coli* bacteria colonies on a culture medium at four different substrate concentrations; (a) control, (b) compound **1**. (1): 24.7 mmol L⁻¹; (2): 52.9 mmol L⁻¹; (3): 105.9 mmol L⁻¹; (4): 211.8 mmol L⁻¹; (c) [PMe₄]I. (1): 26.7 mmol L⁻¹; (2): 57.3 mmol L⁻¹; (3): 114.6 mmol L⁻¹; (4): 229.3 mmol L⁻¹; (d) [P(CH₂OH)₄]SO₄. (1): 1.35 mmol L⁻¹; (2): 2.71 mmol L⁻¹; (3): 5.42 mmol L⁻¹; (4): 10.8 mmol L⁻¹; (e) inhibited colony growth of control, NaI, **1**, [PMe₄]I and [P(CH₂OH)₄]SO₄.

toxic.^{21,29} According to this, **1** and [PMe₄]I (**7**) are considered as non-toxic ([PMe₄]I being at the limit of non-toxic), whereas THPS is considered as very toxic. Furthermore, the assessment of bactericidal activity on *E. coli* was determined on the basis of the number of colonies formed on a culture medium at four different concentrations of the substrates.²² Due to the low EC₅₀ values for THPS, lower substrate concentrations during the breeding of colonies on the plates were used. As already indicated by the EC₅₀ values, sodium iodide showed no effect on the bacteria within this experiment. Compared with the control sample (a), only [P(CH₂OH)₄]SO₄ for the concentrations 2, 3 and 4 shows lower colony numbers (Fig. 16). This confirms the results obtained in Fig. 15, that only THPS is to be classified as toxic. In Fig. 16 subsection e), the result of additional growth inhibition studies is shown. The results indicate that THPS also inhibits bacterial growth. All other substances used do not inhibit bacterial growth. Based on these investigations it can be concluded that the C-F bond in **1** remains stable despite the stronger enthalpy of HF formation compared to H₂O. This illustrates once more the high metabolic stability of the CH₂F group as compared to the bioisosteric CH₂OH group.^{3b}

Conclusions

In summary, we have reported an efficient and facile synthesis method for a series of new fluoromethyl phosphonium salts in high purity. Single crystal X-ray diffraction gives an insight in the influence of the substituents at the phosphorus on the structural parameters of the P-CH₂F group. The C-F bond length stays unaffected by substitution at phosphorus and corresponds to a typical C-F single bond. The P-C bond length fits well to that reported for bioisosteric P-CH₂OH derivatives. In all cases investigated weak intermolecular H···I and H···F interactions are observed. They have been studied by Hirshfeld analysis. In particular the H···F interactions favor the formation of hydrogen bonded chains in the crystal, which represent the structural motif for the fluoromethyl phosphonium salts **1**, **2** and **4**. The H···I contacts are characteristic for the cation/anion interaction. Toxicological tests were carried out on the most water soluble phosphonium salt **1**. In contrast to the toxic P-CH₂OH structural motif the bioisosteric P-CH₂F group showed no toxicity in the case of the bacteria investigated. This finding is anticipated to be useful for adjusting the toxicity of P-CH₂OH based biocides.

Experimental section

Materials and instruments

All compounds were handled using *Schlenk* techniques under dry argon. The phosphines were obtained from BASF, Hoechst AG and VWR. Fluoroiodomethane was distilled under inert conditions before use. The samples for infrared spectroscopy were placed under ambient conditions without further preparation onto a Smith DuraSamplIR II ATR device and measured with a PerkinElmer BX II FR-IR System spectrometer. Raman spectra was measured with a Bruker MultiRam FT Raman spectrometer. Melting/decomposition points were determined with a OZM DTA 552-Ex instrument. The samples for NMR spectroscopy were prepared under inert atmosphere using Ar as protective gas. The solvent used was dried using 3 Å mol sieve and stored under Ar atmosphere. Spectra were recorded with a Bruker Avance III spectrometer operating at 400.1 MHz (¹H), 376.4 MHz (¹⁹F), 100.6 MHz (¹³C) and 162 MHz (³¹P). Chemical shifts are referred to TMS (¹H, ¹³C), CFCl₃ (¹⁹F) and H₃PO₄ (³¹P). All spectra were recorded at 299.15 K. Mass spectrometric data were acquired with a Jeol MStation sectorfield instrument in the FAB⁺ mode. Elemental burning analysis was performed using an Elementar vario EL instrument. Single crystals, suitable for X-ray diffraction, were obtained by slow evaporation of a solution in acetonitrile. Data collection was performed with an Oxford Xcalibur 3 diffractometer equipped with a Spellman generator (50 kV, 40 mA) and a Kappa CCD detector, operating with Mo-K_α radiation (λ = 0.71073 Å). Data collection and data reduction were performed with the CrysAlisPro software.²³ Absorption correction using the multiscan method²³ was applied. The structures were solved with SHELXS-97,²⁴ refined with SHELXL-97²⁵ and finally checked using PLATON.²⁶

Synthesis and characterization

(Fluoromethyl)trimethylphosphonium iodide (1). Caution, this reaction is very exothermic! Trimethylphosphine (7.06 g, 92.8 mmol) was condensed in a flask and cooled to -78 °C. To this fluoroiodomethane (6.24 mL, 92.8 mmol) was carefully added. After 30 min the reaction mixture was allowed to warm up to ambient temperature. The precipitate was dried *in vacuo* and **1** was obtained as white powder (21.7 g, 0.09 mol, 99%). Phas. trans. 54 °C; 128 °C; Dec. p. 209 °C; ¹H NMR (400 MHz, D₂O, 26 °C): δ = 5.44 (d, ²J_{H,F} = 45.3 Hz, 2H; CH₂F), 2.05 (d, ²J_{H,P} = 15.0 Hz, 9H; CH₃); ¹³C{¹H} NMR (100.6 MHz, D₂O, 26 °C): δ = 77.1 (dd, ¹J_{C,F} = 183.8 Hz, ¹J_{C,P} = 64.6 Hz; CH₂F), 4.9 (d, ¹J_{C,P} = 53.6 Hz; CH₃); ³¹P{¹H} NMR (162 MHz, D₂O, 26 °C): δ = 27.2 (d, ²J_{P,F} = 60.3 Hz); ³¹P NMR (162 MHz, D₂O, 26 °C): δ = 27.2 (d of dezettes of t, ²J_{P,F} = 60.3 Hz, ²J_{P,H} = 15.0 Hz to CH₃, ²J_{P,H} = 1.6 Hz to CH₂F) ¹⁹F{¹H} NMR (376 MHz, D₂O, 26 °C): δ = -242.8 (d, ²J_{F,P} = 60.3 Hz); ¹⁹F NMR (376 MHz, D₂O, 26 °C): δ = -242.8 (dt, ²J_{F,P} = 60.3 Hz, ²J_{F,H} = 45.3 Hz); IR (ATR): $\tilde{\nu}$ = 2993 (s), 2957 (m), 2919 (m), 2899 (m), 2886 (w), 1627 (w), 1567 (w), 1524 (w), 1440 (w), 1418 (w), 1397 (w), 1321 (w), 1304 (w), 1291 (m), 1224 (m), 1021 (s), 962 (s), 883 (s), 809 (m), 779 (m), 745 (w), 643 cm⁻¹ (m); Raman (1000 mW): $\tilde{\nu}$ = 2992 (s), 2958 (s), 2917 (s), 2900 (s), 2889 (s), 2791 (m), 1441 (w), 1418 (w), 1324 (w), 1290 (w), 1225 (w), 1025 (w), 972 (w), 940 (w), 885 (w), 783 (w), 746 (w), 646 (m), 379 (w), 272 (m), 250 cm⁻¹ (w); HRMS (FAB) (*m/z*): calcd for C₄H₁₀FP: 109.0582 [M⁺]; found, 109.0567; elemental analysis calcd (%) for C₄H₁₀FIP: C 20.36 H 4.70; found C 20.40 H 4.66.

Tris(diethylamino)(fluoromethyl)phosphonium iodide (2). Tris(diethylamino)phosphine was synthesized as described in literature.²⁷ To a solution of fluoroiodomethane (0.676 mL, 10.0 mmol) in diethylether (90.0 mL) cooled to 0 °C, a solution of tris(diethylamino)phosphine (2.73 mL, 10.0 mmol) in diethylether (10 mL) was added slowly with stirring during 3 h. The solution was concentrated and cooled to -10 °C. The precipitate was filtrated off and compound **2** was obtained as colorless crystals (3.25 g, 0.008 mol, 80%). M.p. 70 °C; Dec. p. 130 °C; ¹H NMR (400 MHz, CDCl₃, 26 °C): δ = 5.77 (d, ²J_{H,F} = 45.9 Hz, 2H; CH₂F), 3.24 (dq, ³J_{H,P} = 11.2 Hz, ³J_{H,H} = 7.1 Hz, 12H; NCH₂), 1.26 (t, ³J_{H,H} = 7.1 Hz, 18H; CH₃); ¹³C{¹H} NMR (100.6 MHz, CD₃CN, 26 °C): δ = 78.2 (dd, ¹J_{C,F} = 182.6, ¹J_{C,P} = 130.3 Hz; CH₂F), 40.1 (d, ²J_{C,P} = 4.1 Hz, NCH₂), 13.6 (s, CH₃); ³¹P{¹H} NMR (162 MHz, CDCl₃, 26 °C): δ = 48.1 (d, ²J_{P,F} = 59.9 Hz); ¹⁹F{¹H} NMR (376 MHz, CDCl₃, 26 °C): δ = -241.1 (d, ²J_{F,P} = 59.9 Hz); ¹⁹F NMR (376 MHz, CDCl₃, 26 °C): δ = -241.1 ppm (dt, ²J_{F,P} = 59.9 Hz, ²J_{F,H} = 45.9 Hz); FT-IR (ATR): $\tilde{\nu}$ = 2972 (m), 2925 (m), 2887 (m), 2840 (m), 1747 (w), 1643 (w), 1575 (w), 1465 (w), 1449 (w), 1385 (m), 1369 (m), 1292 (s), 1249 (s), 1209 (s), 1153 (s), 1112 (w), 1059 (w), 1016 (s), 971 (s), 928 (w), 801 (m), 764 (w), 704 (w), 625 cm⁻¹ (w); Raman (1000 mW): $\tilde{\nu}$ = 2974 (s), 2929 (s), 2896 (s), 2840 (s), 1451 (m), 1371 (w), 1371 (w), 1294 (w), 1207 (w), 1082 (w), 1023 (w), 981 (w), 953 (w), 928 (w), 795 (w), 625 (w), 412 (w), 316 cm⁻¹ (w); HRMS (FAB): (*m/z*) calcd for C₁₃H₃₂FN₃P: 280.2318 [M⁺], found, 280.2316; elemental analysis calcd (%) for C₁₃H₃₂FIN₃P: C 38.34 H 7.92 N 10.32; found C 37.06 H 8.13 N 10.01.

Tributyl(fluoromethyl)phosphonium iodide (3). To a solution of tributylphosphine (1.92, 9.50 mmol) in diethylether (15.0 mL), fluoroiodomethane (0.650 mL, 9.50 mmol) was added in small portions over a period of 5 min. The solution was heated to 35 °C for 32 h, the precipitate formed was filtrated off, washed with diethylether (2 × 15.0 mL) and dried *in vacuo*. Compound 3 was obtained as white powder (2.34 g, 6 mmol, 68%). M.p. 58 °C; ¹H NMR (400 MHz, CDCl₃, 26 °C): δ = 5.92 (d, ²J_{H,F} = 45.9 Hz, 2H; CH₂F), 2.71–2.56 (m, 6H, CH₂), 1.70–1.45 (m, 12H, CH₂), 1.00 (t, ³J_{H,H} = 7.1 Hz, 9H; CH₃); ¹³C NMR (100.6 MHz, CDCl₃, 26 °C): δ = 76.1 (dd, ¹J_{C,F} = 190.4 Hz, ¹J_{C,P} = 58.1 Hz; CH₂F), 24.1 (d, ²J_{C,P} = 15.4 Hz; PCH₂CH₂), 23.8 (dd, ³J_{C,P} = 4.6 Hz, ⁵J_{C,F} = 0.7 Hz; PCH₂CH₂CH₂), 18.1 (d, ¹J_{C,P} = 44.6 Hz; PCH₂), 13.6 (d, ⁴J_{C,P} = 0.8 Hz; CH₃); ³¹P{¹H} NMR (162 MHz, CDCl₃, 26 °C): δ = 32.8 (d, ²J_{P,F} = 51.6 Hz); ¹⁹F{¹H} NMR (376 MHz, CDCl₃, 26 °C): δ = –247.9 (d, ²J_{F,P} = 51.6 Hz); ¹⁹F NMR (376 MHz, CDCl₃, 26 °C): δ = –247.9 (dt, ²J_{F,P} = 51.6 Hz, ²J_{F,H} = 45.9 Hz); FT-IR (ATR): $\tilde{\nu}$ = 2960 (s), 2934 (m), 2872 (w), 1572 (m), 1463 (m), 1379 (m), 1340 (m), 1313 (m), 1283 (m), 1231 (m), 1208 (m), 1099 (m), 1078 (m), 1011 (w), 968 (m), 916 (m), 866 (m), 801 (m), 746 (m), 712 (m), 661 cm^{–1} (w); Raman (1000 mW): $\tilde{\nu}$ = 2965 (s), 2937 (s), 2904 (s), 2874 (s), 2734 (w), 1447 (m), 1399 (w), 1315 (w), 1100 (w), 1052 (w), 890 (w), 661 (w), 245 cm^{–1} (w); HRMS (FAB): (*m/z*) calcd for C₁₃H₂₉FIP: 235.1985 [M⁺], found, 235.2005; elemental analysis calcd (%) for C₁₃H₂₉FIP: C 43.10 H 8.07; found C 42.97 H 8.05.

Tris(2-cyanoethyl)(fluoromethyl)phosphonium iodide (4). To a solution of tris(2-cyanoethyl)phosphine (0.915 g, 4.74 mmol) in acetonitrile (20.0 mL), fluoroiodomethane (0.350 mL, 4.74 mmol) was added. The solution was stirred for 7 d and then concentrated *in vacuo*. The precipitate was filtrated off and dried *in vacuo*. Crystalline colorless 4 was obtained (1.10 g, 3 mmol, 66%). M.p. 138 °C; ¹H NMR (400 MHz, CD₃CN, 26 °C): δ = 5.85 (d, ²J_{H,F} = 44.8 Hz, 2H; CH₂F), 3.19–2.78 ppm (m, 12H, CH₂); ¹³C NMR (100.6 MHz, CD₃CN, 26 °C): δ = 76.0 (dd, ¹J_{C,F} = 188.3, ¹J_{C,P} = 56.1 Hz; CH₂F), 15.6 (d, ¹J_{C,P} = 46.0 Hz; PCH₂), 11.9; ³¹P{¹H} NMR (162 MHz, CDCl₃, 26 °C): δ = 35.3 (d, ²J_{P,F} = 56.8 Hz); ¹⁹F{¹H} NMR (376 MHz, CDCl₃, 26 °C): δ = –249.5 (d, ²J_{F,P} = 56.8 Hz); ¹⁹F NMR (376 MHz, CDCl₃, 26 °C): δ = –249.5 ppm (dt, ²J_{F,P} = 56.8, ²J_{F,H} = 44.8 Hz); FT-IR (ATR): $\tilde{\nu}$ = 3001 (w), 2958 (m), 2927 (s), 2899 (m), 2251 (s), 1571 (w), 1411 (s), 1362 (s), 1311 (m), 1243 (m), 1229 (m), 1191 (w), 1028 (s), 1005 (m), 978 (s), 940 (m), 880 (w), 804 (s), 781 (s), 707 (m), 690 (m), 675 (m), 516 cm^{–1} (m); Raman (1000 mW): $\tilde{\nu}$ = 2999 (w), 2960 (w), 2923 (s), 2901 (s), 2250 (s), 1411 (w), 1395 (w), 1311 (w), 1246 (w), 1005 (w), 915 (w), 806 (w), 692 (w), 676 (w), 484 (w), 411 (w), 369 (w), 250 (w), 201 cm^{–1} (w); HRMS (FAB): (*m/z*) calcd for C₁₀H₁₄FIN₃P: 226.2146 [M⁺], found, 226.0922; elemental analysis calcd (%) for C₁₀H₁₄FIN₃P: C 34.01 H 4.00 N 11.90; found C 34.12 H 4.10 N 11.90.

5-(Diphenylphosphino)-1-fluoromethyldiphenyl phosphonium iodide (5). 1,1'-(Oxydi-2,1-phenylene)bis(1,1'-diphenylphosphine) (0.30 g, 0.576 mmol) was dissolved in toluene (25.0 mL) and fluoroiodomethane (0.100 mL, 1.5 mmol) was added. The solution was heated to 110 °C for 1 d and the resulting precipitate was filtrated off, washed with toluene (3 × 15.0 mL) and dried *in vacuo* to yield colorless crystals of 5 (0.41 g, 0.58 mmol, 55%).

Dec. p. 231 °C; ¹H NMR (400 MHz, CDCl₃, 26 °C): δ = 7.95–7.89 (m, 2H; ArH), 7.85–7.81 (m, 1H; ArH), 7.79–7.75 (m, 1H; ArH), 7.72–7.61 (m, 8H; ArH), 7.56–7.47 (m, 6H; ArH), 7.44–7.38 (m, 3H; ArH), 7.33–7.29 (m, 2H; ArH), 7.23–7.17 (m, 2H; ArH), 7.03–6.98 (m, 2H; ArH), 6.82–6.79 (m, 1H; ArH), 6.28 ppm (dd, ²J_{H,F} = 46.0, ²J_{H,P} = 12.8 Hz, 2H; CH₂F); Due to the low solubility no ¹³C NMR spectrum of acceptable quality could be obtained. ³¹P{¹H} NMR (162 MHz, CDCl₃, 26 °C): δ = 18.7 (d, ²J_{P,F} = 62.2 Hz; 1P, PCH₂F), 30.7 ppm (s; 1P, PPh₂); ¹⁹F{¹H} NMR (376 MHz, CDCl₃, 26 °C): δ = –240.3 ppm (d, ²J_{F,P} = 62.2 Hz); ¹⁹F NMR (376 MHz, CDCl₃, 26 °C): δ = –240.3 (dt, ²J_{F,P} = 62.2 Hz, ²J_{F,H} = 45.3 Hz); FT-IR (ATR): $\tilde{\nu}$ = 3145 (w), 3048 (w), 2988 (w), 2887 (w), 1580 (m), 1563 (m), 1520 (m), 1475 (s), 1458 (s), 1435 (s), 1342 (w), 1314 (w), 1264 (m), 1233 (s), 1188 (m), 1157 (m), 1133 (w), 1110 (m), 1100 (m), 1076 (w), 1029 (s), 996 (w), 907 (w), 886 (m), 793 (m), 754 (m), 744 (s), 721 (w), 702 (s), 688 (w), 620 (w), 542 (s), 505 cm^{–1} (m); Raman (1000 mW): $\tilde{\nu}$ = 3143 (w), 3051 (s), 2884 (w), 2832 (w), 1584 (s), 1189 (w), 1164 (w), 1110 (w), 1098 (w), 1030 (m), 999 (s), 794 (w), 692 (w), 671 (w), 615 (w), 584 (w), 306 (w), 262 (w), 225 (w), 177 cm^{–1} (w); HRMS (EI): (*m/z*) calcd for C₃₇H₃₀FIOP₂: 698.4964 [M⁺], found, 571.1760; elemental analysis calcd (%) for C₃₇H₃₀FIOP₂: C 63.62 H 4.33; found C 63.91 H 4.36.

(Fluoromethyl)diphenylphosphine (6a). Diphenylphosphine (0.499 mL, 2.87 mmol) was solved in THF (15.0 mL) and cooled to 0 °C. *n*-Butyllithium (2.43 mL, 1.30 M, 3.16 mmol) was added and the solution was stirred for 1 h. The deep red solution was cooled to –78 °C and fluoroiodomethane (0.194 mL, 2.87 mmol) was added in portions over a period of 10 min. The reaction mixture was allowed to warm up to ambient temperature overnight. Degassed water (0.50 mL) was added and THF was removed *in vacuo*. The product was extracted with pentane (15.0 mL) and the solvent removed *in vacuo*. A colorless oil was obtained. (0.41 g, 2 mmol, 65%). M.p. –32 °C; Dec. p. 235 °C; ¹H NMR (400 MHz, CDCl₃, 26 °C): δ = 7.54–7.47 (m, 4H; ArH), 7.41–7.34 (m, 6H; ArH), 5.28 (dd, ²J_{H,F} = 49.0 Hz, ²J_{H,P} = 8.4 Hz, 6H; CH₂F); ¹³C NMR (100.6 MHz, CDCl₃, 26 °C): δ = 133.5 (dd, ¹J_{C,P} = 17.7 Hz, ³J_{C,F} = 0.8 Hz; C-*i*), 129.3, 128.7, 128.6, 84.6 (dd, ¹J_{C,F} = 199.9, ¹J_{C,P} = 21.3 Hz; CH₂F); ³¹P{¹H} NMR (162 MHz, CDCl₃, 26 °C): δ = –11.9 (d, ²J_{P,F} = 114.0 Hz); ¹⁹F{¹H} NMR (376 MHz, CDCl₃, 26 °C): δ = –230.4 (d, ²J_{P,F} = 114.0 Hz); ¹⁹F NMR (376 MHz, CDCl₃, 26 °C): δ = –230.4 (dt, ²J_{F,P} = 114.0, ²J_{F,H} = 49.0 Hz); FT-IR (ATR): $\tilde{\nu}$ = 3054 (m), 2918 (s), 1958 (m), 1889 (m), 1809 (m), 1586 (m), 1481 (m), 1433 (m), 1306 (m), 1236 (m), 1184 (m), 1123 (m), 1096 (m), 1069 (m), 977 (m), 914 (w), 843 (m), 740 (w), 721 (m), 691 (m), 618 (m), 544 (m), 506 cm^{–1} (m); Raman (1000 mW): $\tilde{\nu}$ = 3142 (s), 3056 (m), 2958 (m), 2919 (m), 1587 (m), 1572 (w), 1435 (w), 1186 (w), 1159 (w), 1099 (w), 1029 (m), 1000 (s), 684 (w), 668 (w), 618 (w), 377 (w), 262 (w), 204 cm^{–1} (w); HRMS (EI): (*m/z*) calcd for C₁₃H₁₂FP: 218.2112 [M⁺], found 218.0653; elemental analysis calcd (%) C₁₃H₁₂FP: C 71.56 H 5.54; found C 71.74 H 5.78.

Determination of TEP value. Ni(CO)₄ (1.56 g, 9.17 mmol) was condensed into a flask and pentane (25 mL) was added. The solution was cooled to –78 °C and a solution of (fluoromethyl)-diphenylphosphine (0.20 g, 0.91 mmol) in pentane (10 mL) was slowly added. The reaction mixture was warmed to room

temperature within 2 h, the solvent and the excess of Ni(CO)₄ were removed *in vacuo* and a colorless solid was obtained. FT-IR-TEP (ATR): $\tilde{\nu}$ = 3060 (m), 2919 (m), 2068 (s), 1988 (m), 1943 (m), 1568 (m), 1488 (m), 1431 (m), 1334 (m), 1100 (m), 995 (m), 850 (m), 798 (m), 745 (m), 737 (m), 689 cm⁻¹ (m).

Reaction of fluoroiodomethane with (fluoromethyl)diphenyl phosphine

Freshly prepared fluoromethyldiphenyl phosphine (0.41 g, 1.88 mmol) was dissolved in toluene (20.0 mL) and fluoroiodomethane (0.127 mL, 1.88 mmol) was added dropwise at ambient temperature. The reaction mixture was stirred over night. The ³¹P{¹H} NMR spectrum showed no indication for the formation of bis(fluoromethyl)diphenyl phosphonium iodide. The reaction mixture was heated to reflux for 1 d. Again the ³¹P{¹H} NMR spectrum showed no indication for the formation of bis(fluoromethyl)diphenyl phosphonium iodide; instead in addition to the starting phosphine **6** the formation of small amounts of some unidentified phosphorus containing products ($\delta^{31}\text{P} = 45\text{--}22$) was observed. Applying an analogous procedure no reaction was observed also when using diethyl-ether and acetonitrile as solvents.

Conflicts of interest

There are no conflicts to declare.

Acknowledgements

Financial support by Ludwig-Maximilian University is grateful acknowledged. We are thankful to F-Select GmbH for a generous donation of fluoroiodomethane. The authors thank Prof. Dr T. M. Klapötke, Ludwig-Maximilian University, for the generous allocation of diffractometer time. Dr Peter Mayer is thanked, for the help of solving the crystal structure of compound **1**.

Notes and references

- (a) G. Wittig and W. Haag, *Chem. Ber.*, 1955, **88**, 1654–1666; (b) G. Wittig and U. Schöllkopf, *Chem. Ber.*, 1954, **87**, 1318–1330; (c) H. Schmidbaur, *Inorg. Synth.*, 1978, **18**, 135–140.
- Y. L. Yagupolskii, N. V. Pavlenko, S. V. Shelyazhenko, A. A. Filatov, M. M. Kremlev, A. I. Mushta, I. I. Gerus, S. Peng, V. A. Petrov and M. Nappa, *J. Fluorine Chem.*, 2015, **179**, 134–141.
- (a) M. Reichel, J. Martens, E. Woellner, L. Huber, A. Kornath and K. Karaghiosoff, *Eur. J. Inorg. Chem.*, 2019, 2530–2534; (b) J. Hu, W. Zhang and F. Wang, *Chem. Commun.*, 2009, 7465–7478.
- J. Hu, B. Gao, L. Li, C. Ni and J. Hu, *Org. Lett.*, 2015, **17**, 3086–3089.
- (a) N. A. Meanwell, *J. Med. Chem.*, 2018, **61**, 5822–5880; (b) N. A. Meanwell, *J. Med. Chem.*, 2011, **54**, 2529–2591;
- (c) G. A. Showell and J. S. Mills, *Drug Discovery Today*, 2003, **8**, 551–556.
- (a) C. C. Okoro, *Pet. Sci. Technol.*, 2015, **33**, 1366–1372; (b) Y. Xue and G. Voordouw, *Front. Microbiol.*, 2015, **6**, 1387; (c) P. Bajpai, *Pulp and Paper Industry: Microbiological Issues in Papermaking*, Elsevier Science, 2015.
- (a) S. P. Denyer, *Int. Biodeterior. Biodegrad.*, 1995, **36**, 227–245; (b) A. Kanazawa, T. Ikeda and T. Endo, *J. Appl. Bacteriol.*, 1995, **78**, 55–60.
- M. Pohanka, *Biomed. Pap.*, 2011, **155**, 219–230.
- (a) T. Liang, C. N. Neumann and T. Ritter, *Angew. Chem., Int. Ed.*, 2013, **52**, 8214–8264 (*Angew. Chem.*, 2013, **125**, 8372–8423); (b) P. Kirsch, *Modern Fluoroorganic Chemistry: Synthesis, Reactivity, Applications*, Wiley, 2006.
- (a) C. A. Tolman, *Chem. Rev.*, 1977, **77**, 313–348; (b) D. G. Gusev, *Organometallics*, 2009, **28**, 6458–6461; (c) G. Landelle and J.-F. Paquin, *e-EROS Encyclopedia of Reagents for Organic Synthesis*, John Wiley & Sons, Ltd, Chichester, UK, 2011, pp. 1–2.
- (a) W. V. E. Doering and A. K. Hoffmann, *J. Am. Chem. Soc.*, 1955, **77**, 521–526; (b) L. V. Nesterov, A. Y. Kessel and R. I. Mutalapova, *Zh. Obshch. Khim.*, 1969, **39**, 2453–2456; (c) W. C. Davies and W. J. Jones, *J. Chem. Soc.*, 1929, 33–35; (d) M. M. Rauhut, I. Hechenbleikner, H. A. Currier, F. C. Schaeffer and V. P. Wystrach, *J. Am. Chem. Soc.*, 1959, **81**, 1103–1107.
- (a) D. J. Burton and D. M. Wiemers, *J. Fluorine Chem.*, 1985, **27**, 85–89; (b) R. Mazurkiewicz, T. Gorewoda, A. Kuznik and M. Grymel, *Tetrahedron Lett.*, 2006, **47**, 4219–4220.
- G. Prakash, I. Ledneczki, S. Chacko and G. A. Olah, *Org. Lett.*, 2008, **10**, 557–560.
- (a) F. H. Allen, O. Kennard, D. G. Watson, L. Brammer, A. G. Orpen and R. Taylor, *J. Chem. Soc., Perkin Trans. 2*, 1987, 1–19; (b) A. Kornath, F. Neumann and H. Oberhammer, *Inorg. Chem.*, 2003, **42**, 2894–2901.
- R.-X. Li, L. Zhou, P.-P. Shi, X. Zheng, J.-X. Gao, Q. Ye and D.-W. Fu, *New J. Chem.*, 2019, **43**, 154–161.
- T. Steiner, *Angew. Chem., Int. Ed.*, 2002, **41**, 48–76 (*Angew. Chem.*, 2002, **114**, 50–80).
- M. C. Davis and D. A. Parrish, *Synth. Commun.*, 2008, **38**, 3909–3918.
- H. Schmidbaur, R. Pichl and G. Mueller, *Z. Naturforsch., B: Anorg. Chem., Org. Chem.*, 1986, **41B**, 395–397.
- (a) X. Shen, M. Zhou, C. Ni, W. Zhang and J. Hu, *Science*, 2014, **5**, 117–122; (b) F. Dornhaus, M. Bolte, H.-W. Lerner and M. Wagner, *Eur. J. Inorg. Chem.*, 2006, 5138–5147.
- N. J. Goodwin, W. Henderson and B. K. Nicholson, *Inorg. Chim. Acta*, 2002, **335**, 113–118.
- (a) Vol. DIN EN ISO 11348-2:2009-05; (b) Vol. DIN EN ISO 11348-1:2009-05.
- P. Broxton, P. M. Woodcock and P. Gilbert, *J. Appl. Bacteriol.*, 1983, **54**, 345–353.
- Program package CrysAlisPro 1.171.38.46 Rigaku OD, 2015.
- G. M. Sheldrick, *SHELXS-97: Program for Crystal Structure Solution*, University of Göttingen, Germany, 1997.

- 25 G. M. Sheldrick, *SHELXL-97: Program for the Refinement of Crystal Structures*, University of Göttingen, Germany, 1997.
- 26 A. L. Spek, *PLATON: A Multipurpose Crystallographic Tool*, Utrecht University, Utrecht, The Netherlands, 1999.
- 27 G. Bencivenni, R. Cesari, D. Nanni, H. El Mkami and J. C. Walton, *Org. Biomol. Chem.*, 2010, **8**, 5097–5104.
- 28 W. T. Pennington, *J. Appl. Crystallogr.*, 1999, **32**, 1028–1029.
- 29 (a) C. J. Cao, M. S. Johnson, M. M. Hurley and T. M. Klapötke, *ANNAF J. Propuls. Energet.*, 2012, **5**, 41–51; (b) T. Backhaus and L. H. Grimme, *Chemosphere*, 1999, **38**, 3291–3301.